Modeling and Analysis of Tiltrotor Whirl Flutter Based on Lagrange Equations of the Second Kind and Transient Perturbation Method

Shuai Zhang Liangjun Li Yiran Gong Tianheng Yao Haowen Wang* Chen Jiang
School of Aerospace Engineering, Tsinghua University, Beijing 100084, China

Abstract

This paper establishes a modeling and analysis framework for tiltrotor whirl flutter based on Lagrange equations of the second kind and the transient perturbation method. A multibody dynamic model is constructed and progressively validated through key subcomponent comparisons, including the gimballed rotor and semispan wing, showing strong agreement with experimental data. The framework accurately predicts the damping trends of the Maryland TiltRotor Rig across different rotor and wing configurations. Additionally, the study confirms that freewheeling mode yields lower damping than constant-speed mode, even under identical collective pitch settings, and identifies the critical roles of wing and blade stiffness, wing–pylon angle, and wing sweep in determining system stability, where reduced wing stiffness may lead to instability, blade stiffness significantly influences chord damping, the wing–pylon angle alters damping trends in different modes, and wing sweep has opposite effects on beam and chord mode damping. The proposed method provides a validated and reliable tool for analyzing tiltrotor aeroelastic behavior and offers guidance for stability-oriented design optimization.

1. NOTATION

Symbols

C	Damping Matrix
K	Stiffness Matrix
M	Mass Matrix
M_z	Rotor Speed of Rotation, rad/s
β	Wing Swept Angle
γ	Wing-pylon Angle
Ω	Rotor Speed of Rotation, rad/s

Acronyms:

MTR	Maryland TiltRotor Rig
TRAST	TiltRotor Aeroelastic Stability Testbed
WRATS	Wing and Rotor Aeroelastic Testing System

* **Corresponding Author.**

2. INTRODUCTION

Tiltrotor, by installing tiltable rotors at both ends of the wings, enables it to retain excellent performance such as efficient vertical takeoff and landing and aerial hovering of helicopters, while also possessing higher cruise speeds and ranges comparable to proprotors. Due to the similarity in configuration to proprotors in airplane mode, tiltrotors encounter the same issue as proprotors at high speeds—whirl flutter. This instability arises from the coupling of the forces and moments of the rotors and the elastic deformation of the wing-pylon structure. However, the instability problem is more severe on tiltrotor due to its larger rotor with more complex rotor hub structures, which are necessary to ensure high hovering efficiency and to enable flight control in helicopter mode.

Extensive experimental studies have been conducted on whirl flutter of tiltrotor, among which the most noteworthy wind tunnel models include the Wing and Rotor Aeroelastic Testing System (WRATS), the TiltRotor Aeroelastic Stability Testbed (TRAST), and the Maryland TiltRotor Rig (MTR). The WRATS is a 1/5-scale aeroelastic model that was used to guide the preliminary and full-scale design of the V-22 tiltrotor (Ref. 1-5). The TRAST is a semispan wing-pylon system with a three-blades rotor based on XV-15 design, which aims to systematically measure and record a set of the model's parameters with test results (Ref. 6-10). The MTR is designed to serve as an experimental platform for conducting fundamental investigations into the aeromechanics of high-speed tiltrotors. It comprises a three-bladed rotor, the hub(gimballed and hingeless), wing-pylon assembly and motor drive (Ref. 11-16).

Considerable analytical research has also been dedicated to understanding and predicting the whirl flutter of tiltrotor (Ref. 8,10,17-34). Tiltrotor is a large-scale, multi-component coupled system with highly nonlinear and non-periodic dynamics, which makes it difficult to simulate. The development of computer and multibody dynamics analysis technologies has enabled the precise modeling of all important subcomponents of tiltrotor aircraft, such as the wing, pylon, and rotor system. Some of the most noteworthy programs/tools that have been utilized for the analysis of whirl flutter in tiltrotor through multi-body dynamics simulation include: Comprehensive Analytical Model of Rotorcraft Aerodynamics and Dynamics (CAMRAD II) (Ref. 8,24), Rotorcraft Comprehensive Analysis System (RCAS) (Ref. 8,30,35), University of Maryland Advanced Rotorcraft Code Version 2 (UMARC II) (Ref. 34,43,40), DYMORE (Ref. 27,30) and MBDyn (Ref. 27). Except for DYMORE and UMARC, which is used in the analysis of aeroelastic stability of tiltrotor, the aforementioned programs all adopt the approach of first calculating the steady-state periodic solution, then performing linearization of the system dynamics equations based on this steady-state solution, and finally conducting eigenanalysis on the linearized dynamics equations to obtain the system's damping.

The transient perturbation method simulates the dynamic response of the system through direct numerical simulation, fully preserving its nonlinear characteristics and enabling the modeling of large-disturbance scenarios (Ref. 38). In contrast, eigenanalysis, which relies on linearized models, is only valid under small perturbations. Additionally, for systems involving complex control logic (such as flight control systems or pilot-in-the-loop operations), eigenanalysis may lose critical dynamics due to linearization simplifications, whereas the transient perturbation method retains the complete control loop (Ref. 39,40). Moreover, eigenanalysis assumes constant system parameters, while the transient perturbation method can accommodate time-varying parameters such as rotor speed variations (Ref. 12,41). Particularly, the transient perturbation method allows for the inclusion of nonlinear aerodynamic models without any approximation or linearization, and it is also closer to experimental testing method by applying periodically varying control inputs. Therefore, when the tiltrotor is in a complex environment or more influencing factors are considered, the transient perturbation method is undoubtedly more suitable than the eigenanalysis of linearized dynamic equations based on steady-state solutions. In terms of the specific implementation of the transient perturbation method, DYMORE uses the prony method, whereas UMARC II can utilize either the moving-block or the prony method to identify system damping based on the system's transient response under specific excitations, such as periodically varying control inputs (Ref. 15,30). However, since the transient perturbation method requires input excitation after obtaining the steady-state solution and uses a time-stepping approach to simulate the system's motion, it undoubtedly takes longer than the eigenanalysis based on the steady-state solution. Therefore, there are still deficiencies in the analysis of the whirl flutter characteristics of tiltrotor under different configuration parameters using UMARC II and DYMORE. Therefore, the analysis of the whirl flutter characteristics of tiltrotor under different configuration parameters using UMARC II and DYMORE is not sufficient.

This paper develops a multibody dynamics model for tiltrotor employing Lagrange equations of the second kind, coupled with a transient perturbation method for aeroelastic stability analysis, specifically whirl flutter. The generalized coordinates and velocities in Lagrange equations of the second kind are directly associated with the system's motion state, which avoids the need to deal with redundant constraint equations in the first class of Lagrange equations. This makes the physical significance of the state variables in the model more intuitive, thereby facilitating understanding and analysis. Additionally, the reduced number of variables in the equations, along with pure differential equations, allows for more efficient numerical integration and optimization algorithms (Ref. 42). This paper also conducted a series of validation and parametric analysis on the established model based on wind tunnel data of MTR, aiming to validate the model's accuracy while contributing new insights to the application of transient perturbation methods for parametric analysis of tiltrotor.

3. COMPONENT MODELING AND VALIDATION

The tiltrotor model studied in this paper is based on the MTR (Ref. 12). It features on optionally powered, hub-interchangeable, three-blade rotor system which is affixed to a semispan wing. This paper initially develops and validates the key substructures of the tiltrotor aircraft, and then integrates them into a unified model as certified modules. This progressive modeling methodology is instrumental in achieving precise aeroelastic simulation of tiltrotor.

3.1. Gimballed Rotor Model

In the current model, the gimbal is modeled as a constant-velocity joint with two degrees of freedom, and the finite element modeling of the blade is based on the 15-degree-of-freedom moderate deformation beam theory. The Camrad data and results from NASA's 1993 test of the XV-15 are used to validate the dynamic characteristics of gimballed rotor model (Ref. 23), as shown in Table 1 and Table 2.

Table 1: Comparison of XV-15 Rotor Frequencies (Nonrotating)

	Reference/Hz	Paper/Hz	Deviation
1st Flap	7.403	7.293	-1.49%
1st Lag	14.207	14.270	0.44%
2st Flap	29.876	29.376	-1.67%
3st Flap	60.926	59.432	-2.45%
2st Lag	85.626	84.720	-0.64%

Table 2: Comparison of XV-15 Rotor Frequencies ($\Omega = 480\ rpm$)

	Reference/Hz	Paper/Hz	Deviation
1st Flap	12.023	12.042	0.16%
1st Lag	14.813	14.970	1.06%
2st Flap	35.920	35.398	-1.45%
3st Flap	66.835	65.806	-1.54%
2st Lag	89.081	86.908	-2.44%

The aerodynamics of the gimballed rotor was modeled using the C81 airfoil table with five aerodynamic panels. The available rotor wake flow field models include uniform inflow, finite state dynamic inflow (Peters/He) and freewake. Earlier research indicates that the rotor induced inflow model contributes little to whirl flutter predictions (Ref. 34). The reason is that the induced velocity is insignificant relative to the forward flight speed, and the wake of rotor dissipates quickly under the influence of the high-speed freestream. So uniform inflow is a reasonable choice for saving computational effort. In order to verify the accuracy of the rotor aerodynamic model and facilitate the subsequent calculation of tiltrotor whirl flutter prediction, the freewheeling collective predicted by this paper was compared with the experimental results and program prediction results provided by Maryland (Ref. 12). Due to the availability of detailed blade section parameters and airfoil tables in Maryland's study, the predicted collective in this study show excellent agreement with those from Maryland, as shown in Figure 1 and Figure 2.

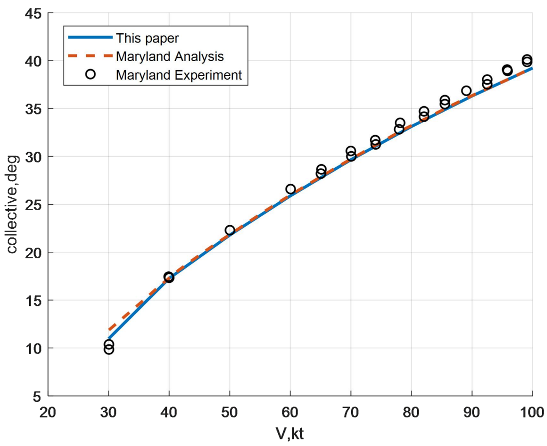

Figure 1: Comparison of freewheeling collective predictions with Maryland's experiment and prediction results at 1050 rpm (straight blade)

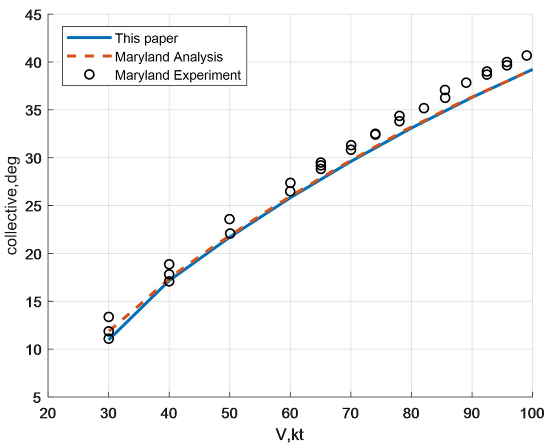

Figure 2: Comparison of freewheeling collective predictions with Maryland's experiment and prediction results at 1050 rpm (swept-tip blade)

3.2. Wing Model

Similarly, a 15-degree-of-freedom moderate deformation beam model is used for the finite element modeling of the wing, with the wing root fixed and constrained to simulate the experiment. The calculated modal frequencies are presented in Table 3. The wing has seven aerodynamic panels, and aerodynamic calculations are based on C81 airfoil decks.

Table 3: Frequencies Comparison of MTR Wing

	Reference/Hz	Paper/Hz	Deviation
1st Flap	5.1	5.07	0.6%
1st Lag	9.7	9.66	0.4%
1st Torsion	14.4	14.60	-1.4%

MTR only provides the structural damping and mode shape corresponding to the three modes in Table 3. Based on the damping values of the above there modes, this paper employs a Caughey damping model retained up to the second order (the following formula) to construct the damping matrix for the wing through finite element modeling.

(1) $$[\mathbf{C}] = a_0[\mathbf{M}] + a_1[\mathbf{K}] + a_2[\mathbf{K}][\mathbf{M}]^{-1}[\mathbf{K}]$$

The three coefficients are determined such that the damping values at the corresponding modal frequencies match the reference values, effectively simulating the wing's internal structural damping. The damping-frequency curve corresponding to the Caughey damping model is shown in Figure 3, where the damping at the above three frequencies matches the reference values.

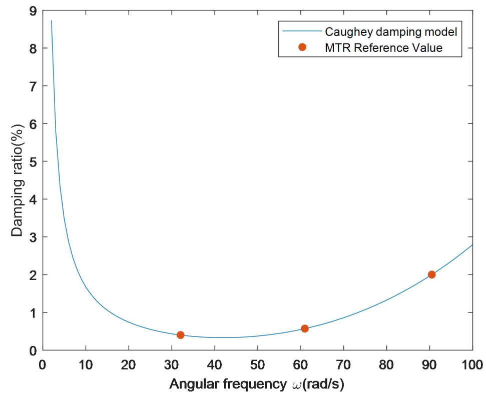

Figure 3: Damping-Frequency Curve of Caughey damping model

3.3. Wing & Rotor Coupled Modeling

After completing the basic modeling of each subcomponent, the simulation calculations based on Lagrange equations of the second kind yield the tangent matrices (including mass, damping, and stiffness matrices) and generalized forces corresponding to the generalized coordinates of each sub-component at the current moment. Pure differential equations of tiltrotor are constructed using these tangent matrices and generalized forces. Subsequently, it is necessary to couple all the sub-components together to obtain the dynamic equations of the entire system. The coupling of the wing and rotor requires considering the influence of the wing's motion on the rotor's inflow and the impact of the rotor's aerodynamic forces and moments on the wing's deformation.

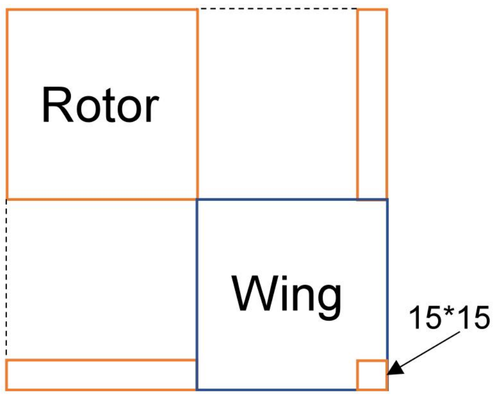

Figure 4: Schematic Diagram of the System Matrix Composed of Wing and Rotor

This paper adds an additional 15 degrees of freedom to all blade elements, corresponding to the 15 elastic degrees of freedom of the wingtip element:

(1) By copying the values corresponding to the elastic 15 degrees of freedom of the wingtip to the additional 15 degrees of freedom of the blade elements, the influence of the wing's motion on the rotor's position and velocity can be transmitted; (2) As shown in Figure 4, the row and column numbers of the tangent matrix calculated from the rotor system composed of blade elements are increased by 15. The 15*15 small matrix in the rotor is directly added to the corresponding matrix block of the wing element, and the remaining coupled parts are directly moved to the position corresponding to the degrees of freedom of the wing element, thereby transmitting the rotor's forces to the wingtip.

3.4. Transient Perturbation Method

The transient perturbation method involves initially applying an external excitation to the system to excite a specific mode. After the excitation is removed, the damping of the corresponding mode is identified by analyzing the free response of the system using moving-block method (Ref. 36).

To verify the computational accuracy of the transient perturbation excitation method and damping recognition in the program, the ITR hingeless rotor was used for calculations, and the results were compared with experimental data (Ref. 37) and the computational results from the UMARC (Ref. 43), as shown in Figure 5.

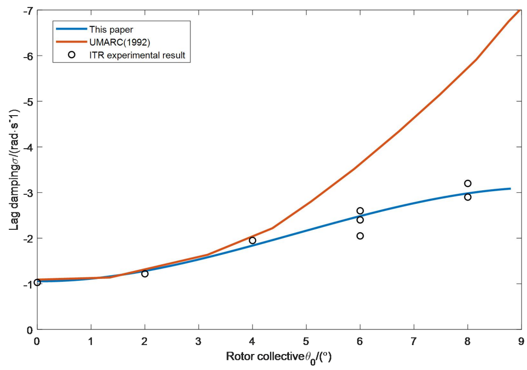

Figure 5: Damping Result Comparison with Experiment and UMARC(1994)

The excitation method for MTR used in this paper is to periodically change the blade pitch input, with specific methods referring to experimental data: the longitudinal cyclic pitch is changed by 5.4° for beam mode; the collective pitch is changed by 2° for chord mode; the longitudinal cyclic pitch is changed by 0.1° for torsion mode.

4. MTR VALIDATION

The University of Maryland not only presented wind tunnel test results and their corresponding predictive analyses, but also supplied detailed parameter configurations for the MTR, including the geometric properties, structural parameters, and airfoil profiles of both the rotors and wings. By providing this comprehensive dataset, they established a benchmark for validation in subsequent researchers' analyses of whirl flutter, which significantly advanced the study of whirl flutter in tiltrotor aircraft.

In 2021, the MTR was tested at the Navy Carderock tunnel with two blade configurations: straight (baseline) and swept-tip (Ref. 12, 14). In addition to the blade configurations, the MTR was evaluated under multiple operational conditions during testing, including: gimbal states (free/locked), wing fairings options (on/off) and drive modes (freewheeling/powered). The baseline configuration of MTR is gimbal-free, with wing fairings on, in freewheeling mode, and equipped with straight and swept-tip blades. Sub-sequent analysis will focus on damping predictions for both straight and swept-tip blades with varying wing fairing configurations due to their substantial effects on damping results. All other test conditions maintained baseline's parameters (gimbal-free, freewheeling).

4.1. Configuration: Wing Fairings On

Figure 6 presents the comparison of wing's beam and chord mode damping prediction for both straight and swept-tip blade configurations with Maryland's analysis result and test data. Comparative validation reveals strong consistency among the present numerical predictions, Maryland's computational results, and experimental data. Key findings include:

(1) Remarkable agreement (<0.05% damping predictions deviation) in beam mode damping predictions;

(2) Systematic 0.2% upward shift in our chord mode damping predictions for straight-blade configurations;

(3) Enhanced smoothness characteristics in our chord mode damping curves.

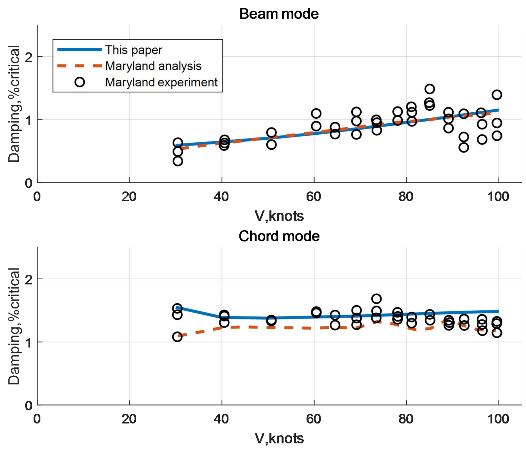

(a) Straight

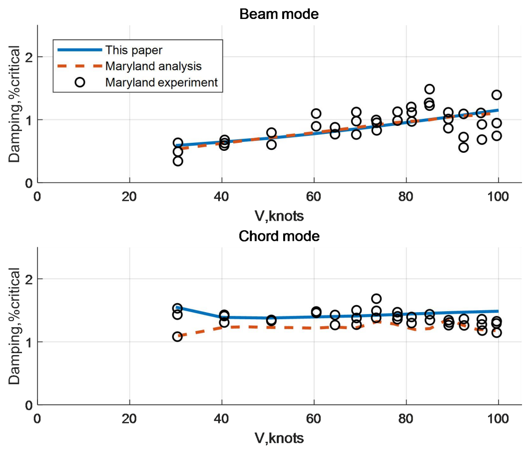

(b) Swept-tip

Figure 6: Comparison of Damping Predictions with Maryland's Prediction and Experiment Data (wing fairings on)

4.2. Configuration: Wing Fairings Off

The removal of wing fairings primarily affects the analytical model in two key aspects:

(1) Significant changes in inertial parameters at wing sections previously covered by fairings, with mass per length reduced by approximately 50% and moment of torsion moment of inertia decreased by two orders of magnitude;

(2) Discontinuation of wing aerodynamic force calculations.

As shown in Figure 7, our predictions maintain excellent agreement with both Maryland's computational results and experimental trends. Comparative analysis with Figure 6 reveals significant decreases in predicted beam mode damping for both straight and swept-tip blade configurations, with a maximum discrepancy of 0.35% occurring at 100 knots. To investigate the relative importance of the two primary factors following fairing removal, we conducted hypothetical computational cases maintaining the original wing aerodynamic model (shown as yellow dash-dotted curves in Figure 7). The results clearly demonstrate that the elimination of wing aerodynamic forces constitutes the dominant influencing factor.

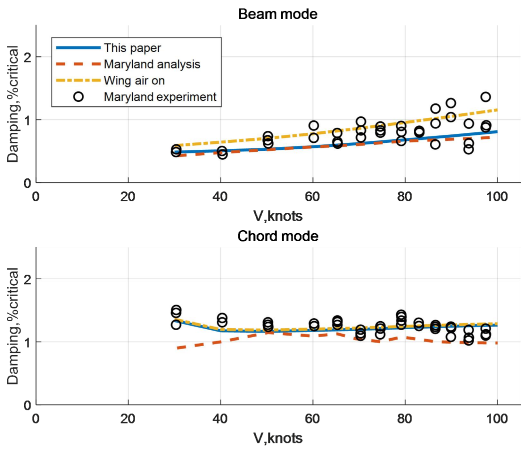

(a) Straight

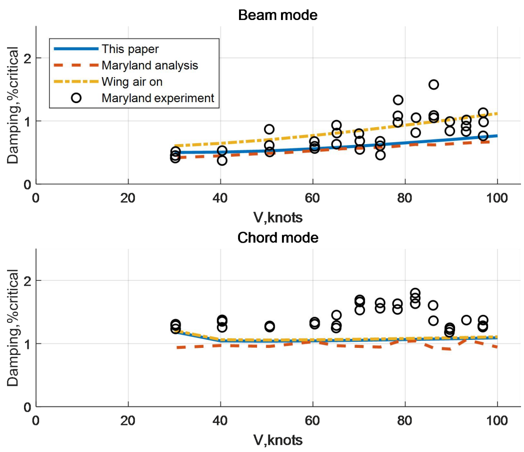

(b) Swept-tip

Figure 7: Comparison of Damping Predictions with Maryland's Prediction and Experiment Data (wing fairings off)

5. PARAMETRIC ANALYSIS

5.1. Freewheeling vs Constant Rotor Speed

Freewheeling means an unpowered rotor system with unconstrained rotational freedom that dynamically adjusts its speed during both forced excitation and free response phases to continuously maintain the zero torque condition about the rotor shaft ($M_z = 0$).

As previously mentioned, the MTR test configuration included both freewheeling and powered modes. Experimental results and corresponding predictions under gimbal-locked and fairings-off conditions from Maryland indicate that the powered mode leads to increased damping in both beam and chord modes compared to the freewheeling mode.

However, under identical wind speed conditions, the powered mode employed different collective compared to the freewheeling mode to approximate representative collective of the flight condition in the experiment. In this study, a model was constructed with the same collective as the freewheeling mode and a constant rotational speed of 1050 rpm to investigate the influence of constant speed mode versus freewheeling mode on damping under identical collective. To enhance the reliability of our conclusions, two significantly different configurations were selected: straight blades with wing fairings on and swept-tip blades with wing fairings off. The results are shown in Figure 8.

It can be observed that even at the same collective, the freewheeling mode exhibits lower wing damping compared to the powered mode due to the release of rotational degrees of freedom:

(1) The damping of the beam mode decreases more significantly as wind speed increases;

(2) The damping of the chord mode is approximately 0.5% lower overall.

The above conclusions indicate that the release of rotational freedom also significantly affects the damping characteristics of gimballed tiltrotors, which is consistent with the findings of the University of Maryland regarding the influence of rotor speed perturbation and constant rotational speed on the whirl flutter characteristics of swept-tip hingeless tiltrotors (Ref. 34).

We attribute this phenomenon to the fact that the rotor-wing/pylon motion during the free response phase (after excitation removal) results in a non-zero rotor shaft torque (M_z) in the constant speed mode, and this torque dissipates energy from the system through rotor rotation, thereby increasing the overall damping.

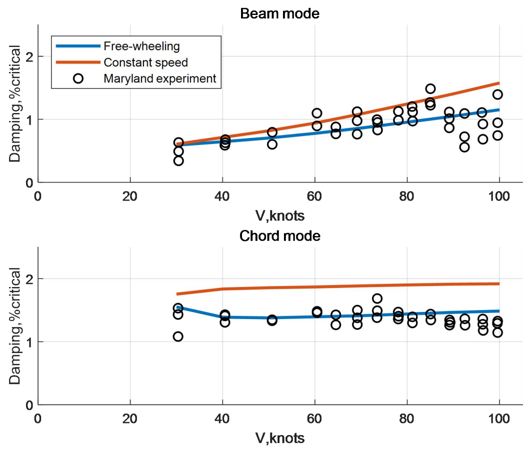

(a) Straight, wing fairings on

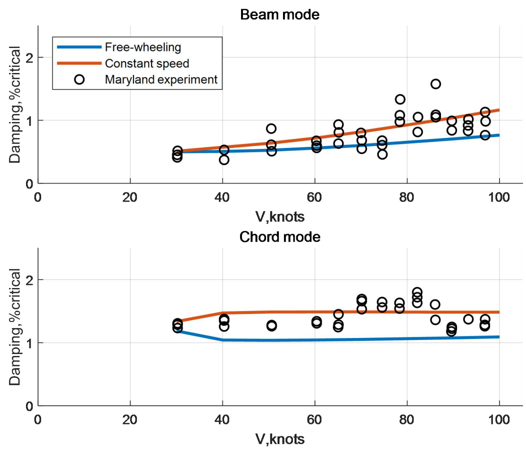

(b) Swept-tip, wing fairings off

Figure 8: Comparison of Damping Predictions of Freewheeling Mode and Constant Rotor Speed Mode in Different Configuration

5.2. Wing Stiffness

The direct installation of the heavy pylon and rotor at the wingtip necessitates adequate wing stiffness to ensure system stability. Based on the MTR baseline configuration, this study investigates the influence of varying wing stiffness on damping prediction.

Notably, in this analysis, the comparison is based on the actual damping corresponding to the modes rather than the damping ratio. This is because variations in wing stiffness can significantly affect the modal frequencies, thereby influencing the analytical conclusions. As illustrated in Figure 9, the damping ratio of the beam mode significantly increases under 0.5 times the normal wing stiffness. This occurs because the reduction in normal stiffness leads to a substantial increase in the period time of the beam mode. However, the decrease in normal stiffness results in only a minor reduction in the energy dissipated per unit time by the system. Consequently, the energy dissipated over one cycle increases markedly, leading to an elevated damping ratio. Moreover, when the wing's normal stiffness is reduced to 0.2 times the baseline value, the system exhibits instability.

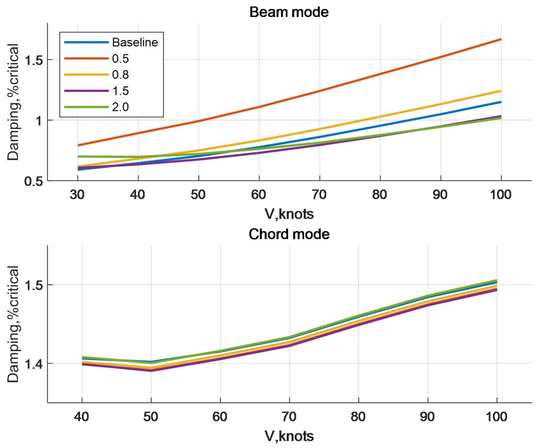

Figure 9: The Influence of Wing Normal Stiffness Variation on Damping Ratio

Figure 10 compares the effects of stiffness variations in three wing directions on wing damping within the 0–100 knot speed range. As shown in Figure 10 (a), reducing the wing's normal stiffness decreases the damping of the beam mode, while increasing it enhances the damping—a trend consistent with physical intuition. In contrast, variations in normal stiffness exhibit negligible influence on the damping of the chord mode.

Figure 10(b) reveals that chordwise stiffness variations also have minimal impact on the beam mode's damping. However, their effect on the chord mode's damping is notably counterintuitive: doubling the stiffness significantly increases the damping, while halving it markedly reduces the damping, whereas intermediate stiffness variations demonstrate an opposing trend.

Figure 10(c) indicates that changes in torsional stiffness primarily affect the chord mode's damping, which decreases with reduced torsional stiffness. Furthermore, as torsional stiffness increases, the chord mode's damping asymptotically approaches a critical threshold, suggesting diminishing returns beyond a certain stiffness level.

The above conclusions are consistent with the findings of Johnson et al. (Ref. 46) in their analysis of the influence of wing structural parameters on a large civil tiltrotor equipped with a four-bladed hingeless rotor. However, their results were presented in terms of damping ratio variations with respect to stiffness (which also exhibit similarity to Figure 9) and require combined analysis with the accompanying modal frequency variation diagram.

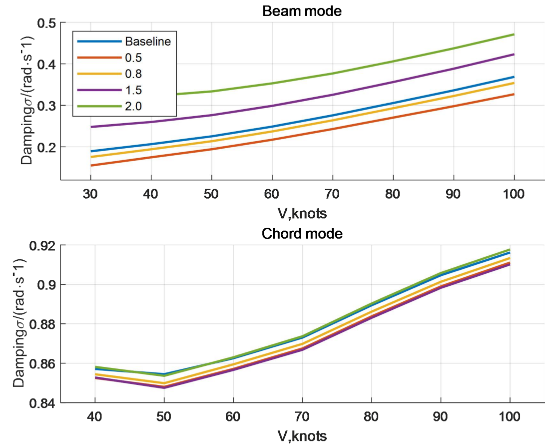

(a) Wing normal stiffness

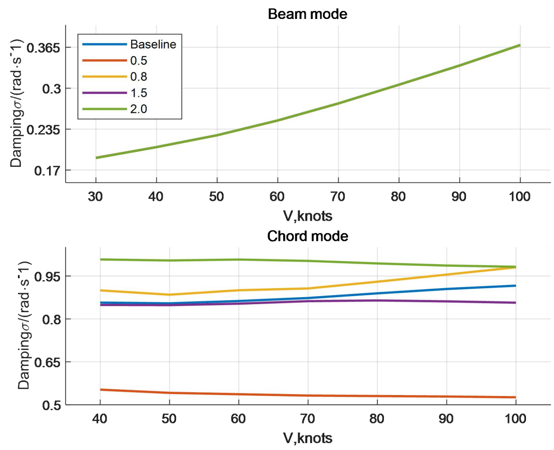

(b) Wing chordwise stiffness

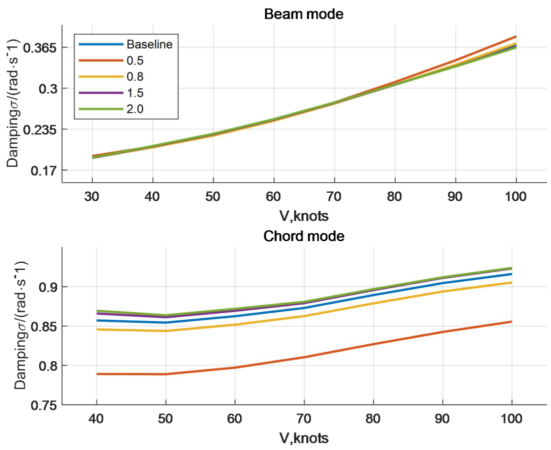

(c) Wing torsional stiffness

Figure 10: The Influence of Wing Stiffness Variation on Actual Damping

5.3. Blade Stiffness

Similarly, the influence of blade stiffness variations on wing modal damping also warrants investigation. Figure 11 compares the effects of blade stiffness variations on the wing damping ratio. Given that changes in blade stiffness have negligible influence on wing modal frequencies, the analysis focuses solely on damping ratios.

As illustrated in Figure 11(a), variations in blade beamwise stiffness exhibit a limited impact on the damping ratio of the wing beam mode. At 0.2× and 0.5× beamwise stiffness, the damping curve of the beam mode displays an upward convex trend within the 80–90 knot range, whereas the baseline and higher stiffness cases retain an overall downward concave trend. Conversely, for the wing chord mode, the damping ratio increases with higher beamwise stiffness.

Figure 11(b) indicates that blade chordwise stiffness variations have a marginal effect on the wing beam mode damping ratio, though a discernible trend emerges: lower chordwise stiffness corresponds to a reduced damping ratio in the beam mode. Similarly, the damping ratio of the wing chord mode decreases with diminishing chordwise stiffness which is more evidently.

Figure 11(c) demonstrates that the damping ratios of both the wing beam and chord modes remain largely insensitive to changes in blade torsional stiffness.

The present analysis agrees with Johnson et al.'s study regarding the consistent influence of blade beamwise and torsional stiffness variations on wing damping characteristics. However, unlike their findings, this study did not observe a noticeable increase in beam mode damping ratio when reducing blade chordwise stiffness; instead, the effect was marginal. This discrepancy may stem from differences in the specific models analyzed, as Johnson et al.'s study indicates that when the blade chordwise stiffness increases, there exists a region where the damping ratio of the beam mode remains almost constant (Ref. 46).

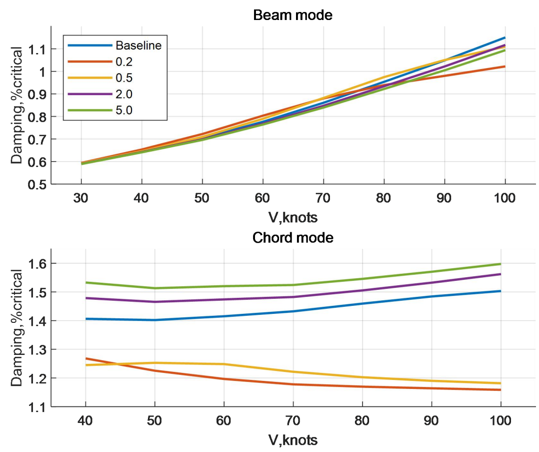

(a) Blade beamwise stiffness

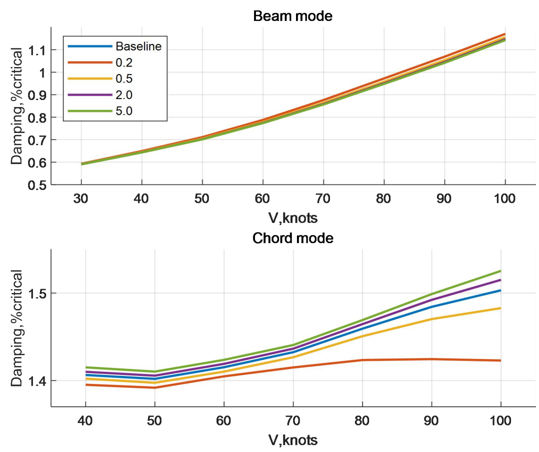

(b) Blade chordwise stiffness

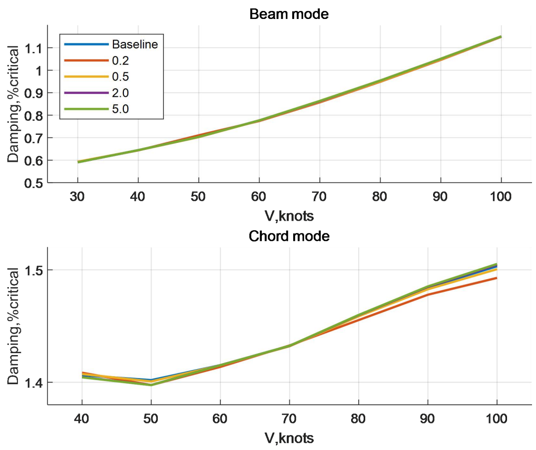

(c) Blade torsional stiffness

Figure 11: The Influence of Blade Stiffness Variation on Damping Ratio

5.4. Wing-pylon Angle

In airplane mode, tiltrotor aircraft typically orient their rotors forward to effectively utilize rotor thrust. However, this configuration may exhibit poorer controllability and stability in yaw and roll during helicopter mode and the transition phase. This study investigates a configuration with an angle γ between the wing and pylon, as illustrated in Figure 12. Such a design may offer improved yaw and roll stability during hover and low-speed flight, similar to the characteristics observed in synchropter aircraft.

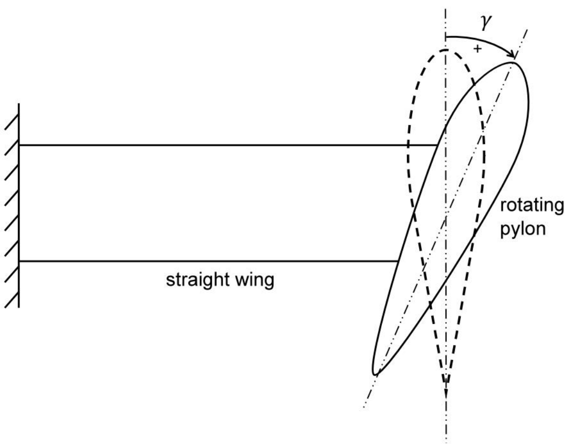

Figure 12: Schematic Diagram of Wing-pylon Angle (clockwise rotation is positive)

Figure 13 demonstrates that regardless of whether the wing-pylon angle is positive or negative, it reduces the damping ratio of the wing beam mode. In contrast, for the chord mode, a more positive wing-pylon angle increases the damping, while a more negative angle decreases it.

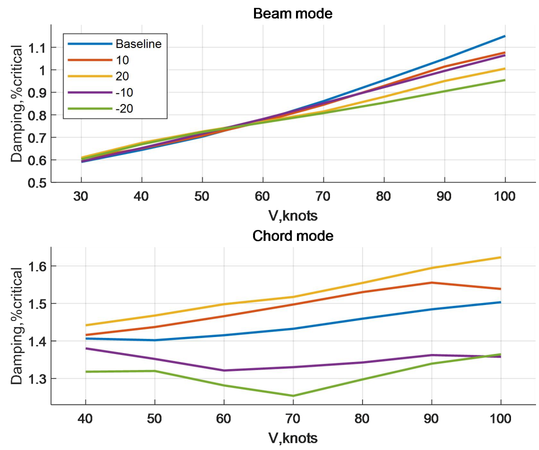

Figure 13: The Influence of Wing-Pylon Angle on Damping Ratio

5.5. Wing Swept

To reduce the aerodynamic interference between the rotor and the wing in airplane mode, the wing is typically designed with a certain forward sweep angle, such as the XV-15 tiltrotor. As illustrated in Figure 14, the wing exhibits a positive sweep angle β, while the wing span remains unchanged to avoid exacerbating instability. The rotor orientation is maintained to ensure sufficient thrust generation. This study subsequently calculates and analyzes the influence of the wing sweep angle on the actual damping of wing modes.

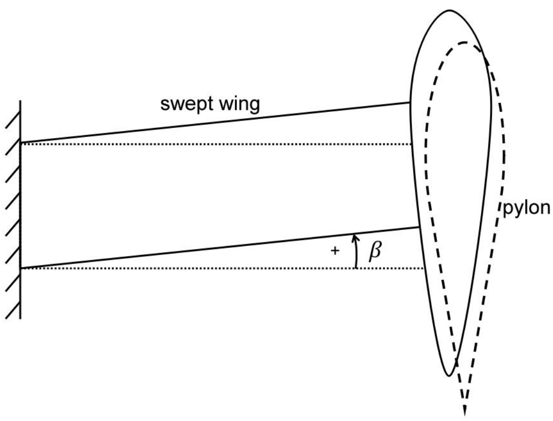

Figure 14: Schematic Diagram of Wing Swept (counterclockwise rotation is positive)

As shown in Figure 15, the forward sweep of the wing generally increases the damping of the beam mode while reducing the damping of the chord mode. Conversely, the backward sweep of the wing decreases the damping of the beam mode but enhances the damping of the chord mode. Both effects become more pronounced with increasing sweep angles. This indicates that wing sweep redistributes the energy dissipation ratio between the beam mode and the chord mode. Therefore, during high-speed flight, adjusting the wing swept angle can be utilized to reduce the damping of a stable mode, thereby increasing the damping of the critical mode.

The aforementioned conclusion is somewhat inconsistent with the findings of Machowski in their study on the effect of wing forward-sweep angle on the speed of whirl flutter. They pointed out that as the forward-sweep angle increases, the critical flutter speeds of both the beam mode and chord mode decrease, whereas the critical flutter speed of the torsion mode increases. This discrepancy may arise from differences in the specific models analyzed. Nevertheless, Machowski's study also demonstrates the influence of wing sweep angle on energy dissipation characteristics (Ref. 45).

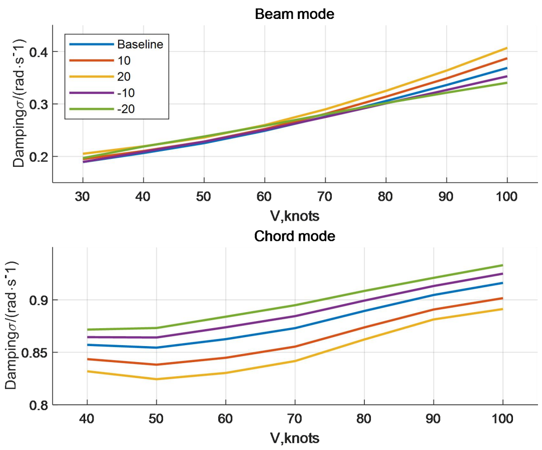

Figure 15: The Influence of Wing Swept on Damping Ratio

6. CONCLUSION

A modeling and analysis framework for tiltrotor aeroelastic stability was developed based on Lagrange equations of the second kind, which avoids the need for constraint equations and enables efficient numerical computation. The model was incrementally validated through sub-system-level verifications (including gimballed rotor and wing models) and demonstrated strong agreement with experimental data. The transient perturbation method was also implemented and validated, confirming its accuracy and feasibility for damping identification near the whirl flutter boundary. The key conclusions are as follows:

1. The model accurately predicted the damping behavior of different rotor and wing configurations, including straight and swept-tip blades and wing fairing effects. The elimination of wing aerodynamic forces was identified as the dominant factor affecting damping when wing fairings are removed.
2. Freewheeling mode produces lower damping than constant-speed mode under identical collective settings.
3. Wing normal stiffness has a dominant influence on beam mode damping and system stability; overly reduced stiffness may lead to instability.
4. Chordwise and torsional stiffness variations significantly affect chord mode damping, while beamwise stiffness mainly impacts beam mode damping.
5. Introducing a wing–pylon angle reduces beam mode damping; its effect on chord mode damping depends on the angle direction.
6. Wing sweep has opposite effects on beam and chord modes, with forward sweep enhancing beam mode damping and reducing chord mode damping.

Author contact:

Shuai Zhang zhangs23@mails.tsinghua.edu.cn
Liangjun Li liliangjun2006@126.com
Yiran Gong yrgong@outlook.com
Tianheng Yao yth21@mails.tsinghua.edu.cn
Haowen Wang* bobwang@tsinghua.edu.cn
Chen Jiang jc2017@mail.tsinghua.edu.cn

7. REFERENCES

1. Popelka, David, Marc Sheffler, and Jim Bilger. "Correlation of Test and Analysis for the 1/5 - Scale V - 22 Aeroelastic Model." Journal of the American Helicopter Society 32.2 (1987): 21-33.

2. Settle, T. Ben, and David L. Kidd. "Evolution and Test History of the V - 22 0.2 - Scale Aeroelastic Model." Journal of the American Helicopter Society 37.1 (1992): 31-45.

3. Nixon, Mark, et al. "Aeroelastic stability of a soft-inplane gimballed tiltrotor model in hover." 19th AIAA Applied Aerodynamics Conference. 2001.

4. Piatak, David J., et al. "A wind-tunnel parametric investigation of tiltrotor whirl-flutter stability boundaries." America Helicopter Society 57th Annual Forum. 2001.

5. Piatak, David J., et al. "A Parametric Investigation of Whirl - Flutter Stability on the WRATS Tiltrotor Model." Journal of the American Helicopter Society 47.2 (2002): 134-144.5

6. Kreshock, Andrew R., Robert Thornburgh, and Matthew Wilbur. "Overview of the tiltrotor aeroelastic stability testbed." AIAA SCITECH 2022 Forum. 2022.

7. Kreshock, Andrew R., et al. "Development of a new aeroelastic tiltrotor wind tunnel testbed." AIAA Scitech 2019 Forum. 2019.

8. Yeo, Hyeonsoo, et al. "Comparison of CAMRAD II and RCAS predictions of tiltrotor aeroelastic stability." Journal of the American Helicopter Society 63.2 (2018): 1-13.8

9. Yeo, Hyeonsoo, and Andrew R. Kreshock. "Whirl flutter investigation of hingeless proprotors." Journal of Aircraft 57.4 (2020): 586-596.

10. Yeo, Hyeonsoo, Hao Kang, and Andrew R. Kreshock. "Unified modeling of the tiltrotor aeroelastic stability testbed for proprotor whirl flutter." Journal of Aircraft 60.3 (2023): 857-869.10

11. Tsai, Frederick, et al. "Whirl flutter test of the Maryland tiltrotor rig: Overview." AIAA SCITECH 2022 Forum. 2022.

12. Gul, Seyhan, and Anubhav Datta. "Whirl flutter test of the maryland tiltrotor rig: Prediction and validation." AIAA SCITECH 2022 Forum. 2022.12

13. Sutherland, James R., Frederick Tsai, and Anubhav Datta. "Whirl flutter test of the maryland tiltrotor rig: Swept-tip blades." AIAA SCITECH 2022 Forum. 2022.

14. Gul, Seyhan, and Anubhav Datta. "Prediction and Validation of Whirl Flutter Data of the Maryland Tiltrotor Rig." Journal of the American Helicopter Society 69.1 (2024): 1-11.

15. Akinwale, Akinola, and Anubhav Datta. "Understanding High-Speed Aeroelastic Stability of a Gimballed Proprotor." Journal of Aircraft (2025): 1-15.

16. Tsai, Frederick. "Development and Whirl Flutter Test of the Maryland Tiltrotor Rig." Journal of the American Helicopter Society 69.1 (2024): 1-15.

17. Reed III, Wilmer H., and Samuel R. Bland. An analytical treatment of aircraft propeller precession instability. No. NASA-TN-D-659. 1961.

18. Reed, Wilmer H. "Review of propeller-rotor whirl flutter." (1967).

19. Johnson, Wayne. Dynamics of tilting proprotor aircraft in cruise flight. No. NASA-TN-D-7677. 1974.

20. Kvaternik, Raymond George. Studies in tilt-rotor VTOL aircraft aeroelasticity. Diss. Ph. D. Dissertation, June 1973, Case Western Reserve University, Cleveland, Ohio, 1973.

21. Kvaternik, Raymond G., and Jerome S. Kohn. An experimental and analytical investigation of proprotor whirl flutter. No. L-11656. 1977.

22. Barkai, S. M., et al. "Modeling and analysis of tilt-rotor aeromechanical phenomena." Mathematical and computer modelling 27.12 (1998): 17-43.

23. Acree Jr, C. W. An improved CAMRAD model for aeroelastic stability analysis of the XV-15 with advanced technology blades. No. NAS 1.15: 4448. 1993.20

24. Acree Jr, C. W., R. J. Peyran, and Wayne Johnson. Rotor design options for improving XV-15 Whirl-Flutter stability margins. No. NASA/TP-2004-212262. 2004.

25. Srinivas, Venkataraman, and Inderjit Chopra. "Validation of a comprehensive aeroelastic analysis for tiltrotor aircraft." Journal of the American Helicopter Society 43.4 (1998): 333-341.

26. Srinivas, Venkataraman, Inderjit Chopra, and Mark W. Nixon. "Aeroelastic analysis of advanced geometry tiltrotor aircraft." Journal of

the American Helicopter Society 43.3 (1998): 212-221.

27. Masarati, Pierangelo, et al. "Soft‐Inplane Tiltrotor Aeromechanics Investigation Using Two Comprehensive Multibody Solvers." Journal of the American Helicopter Society 53.2 (2008): 179-192.24

28. Shen, Jinwei, et al. "Modeling a stiff-inplane tiltrotor using two multibody analyses: a validation study." ANNUAL FORUM PROCEEDINGS-AMERICAN HELICOPTER SOCIETY. Vol. 64. No. 3. AMERICAN HELICOPTER SOCIETY, INC, 2008.25

29. Zhang, Jianhua, and Edward C. Smith. "Influence of aeroelastically tailored wing extensions and winglets on whirl flutter stability." 2nd Asian/Australian Rotorcraft Forum, ARF 2013 and the 4th International Basic Research Conference on Rotorcraft Technology 2013, IBRCRT 2013. American Helicopter Society International, 2013.

30. Shen, Jinwei, and Hao Kang. "Comparison study of tiltrotor whirl flutter using two rotorcraft comprehensive analyses." Journal of Aircraft 54.2 (2017): 845-850.27

31. Koch, Christopher, and Benedikt Koert. "Including blade elasticity into frequency-domain propeller whirl flutter analysis." Journal of Aircraft 61.3 (2024): 774-784.

32. Cocco, Alessandro, and Alberto Savino. "Tiltrotor whirl-flutter assessment by multifidelity aerodynamic models." AIAA Scitech 2024 Forum. 2024.

33. Thornburgh, Robert P., and Andrew R. Kreshock. "Structural Modeling and Validation of the TiltRotor Aeroelastic Stability Testbed." AIAA SCITECH 2024 Forum. 2024.30

34. Gul, Seyhan, and Anubhav Datta. "Aeroelastic loads and stability of swept-tip hingeless tiltrotors toward high-speed instability-free cruise." Journal of the American Helicopter Society 68.1 (2023): 1-18.

35. Saberi, Hossein, et al. "Overview of RCAS capabilities, validations, and rotorcraft applications." American Helicopter Society 71st Annual Forum, Virginia Beach, VA. 2015.

36. Tasker, F. A., and Chopra, I., “Assessment of Transient Analysis Techniques for Rotor Stability Testing,” Journal of the American Helicopter Society, Vol. 35, No. 1, 1990, pp. 39–50.

37. Sharpe, David L. "A comparison of theory and experiment for aeroelastic stability of a hingeless rotor model in hover." Proceedings of the Integrated Technology Rotor Methodology Assessment Workshop. 1988.

38. Hatziargyriou, Nikos, et al. "Definition and classification of power system stability–revisited & extended." IEEE Transactions on Power Systems 36.4 (2020): 3271-3281.

39. Yazdani, Amirnaser, and Reza Iravani. Voltage-sourced converters in power systems: modeling, control, and applications. John Wiley & Sons, 2010.

40. Muscarello, Vincenzo, and Giuseppe Quaranta. "Structural Coupling and Whirl-Flutter Stability with Pilot-in-the-Loop." Journal of the American Helicopter Society 66.3 (2021): 1-16.

41. Machowski, Jan, et al. Power system dynamics and stability. John Wiley & Sons, 1997.

42. Brenan, Kathryn Eleda, Stephen L. Campbell, and Linda Ruth Petzold. Numerical solution of initial-value problems in differential-algebraic equations. Society for Industrial and Applied Mathematics, 1995.

43. Bir, G., I. Chopra, and R. Ganguli. "University of Maryland advanced rotorcraft Code theory manual." Center for Rotorcraft Education and Research University of Maryland: College Park, MD, USA (1994).34

44. Gul, Seyhan, and Anubhav Datta. "Development of an aeromechanics solver for loads and stability of hingeless tiltrotors." Journal of Aircraft 60.1 (2023): 143-159.

45. Nixon, Mark W. "Parametric studies for tiltrotor aeroelastic stability in highspeed flight." Journal of the American Helicopter Society 38.4 (1993): 71-79.

46. Acree Jr, C. W., and Wayne Johnson. "Aeroelastic stability of the LCTR2 civil tiltrotor." (2008).